JACS
JOURNAL OF THE AMERICAN CHEMICAL SOCIETY
pubs.acs.org/JACS
Article

Engineering a Ligase Binding DNA Aptamer into a Templating DNA Scaffold to Guide the Selective Synthesis of Circular DNAzymes and DNA Aptamers

Yu Yan, Dingran Chang, Yongbin Xu, Yangyang Chang, Qiang Zhang, Quan Yuan, Bruno J. Salena, Yingfu Li,* and Meng Liu*

Cite This: J. Am. Chem. Soc. 2023, 145, 2630−2637
Read Online
ACCESS | Metrics & More | Article Recommendations | Supporting Information

ABSTRACT: Functional nucleic acids (FNAs), such as DNAzymes and DNA aptamers, can be engineered into circular forms for improved performance. Circular FNAs are promising candidates for bioanalytical and biomedical applications due to their intriguing properties of enhanced biological stability and compatibility with rolling circle amplification. They are typically made from linear single-stranded (ss) DNA molecules via ligase-mediated ligation. However, it remains a great challenge to synthesize circular ssDNA molecules in high yield due to inherent side reactions where two or more of the same ssDNA molecules are ligated. Herein, we present a strategy to overcome this issue by first using in vitro selection to search from a random-sequence DNA library a ligatable DNA aptamer that binds a DNA ligase and then by engineering this aptamer into a general-purpose templating DNA scaffold to guide the ligase to execute selective intramolecular circularization. We demonstrate the broad utility of this approach via the creation of several species of circular DNA molecules, including a circular DNAzyme sensor for a bacterium and a circular DNA aptamer sensor for a protein target with excellent detection sensitivity and specificity.

INTRODUCTION

Circular functional nucleic acids (cFNAs) refer to naturally occurring or artificial FNAs (e.g., aptamers, DNA enzymes, ribozymes, and aptazymes) with closed-loop configuration.[1] They offer unique features that include FNA-enabled catalysis and/or molecular recognition, inaccessible by exonucleases (due to the lack of 5′ and 3′ ends), higher thermodynamic stability, programmability for molecular device engineering, and the ability for replication by DNA polymerases in a rolling circle manner. These traits have made them popular choices as building blocks to set up molecular systems for wide-ranging applications in disease therapy, medical diagnosis, biosensing, and DNA nanotechnology.[2−8]

A common approach for circular DNA synthesis is ligase-mediated circularization of linear single-stranded (ss) DNA oligonucleotides that can be chemically synthesized. For example, T4 DNA ligase (T4DL) is widely used to circularize a ssDNA with the assistance of a splint DNA strand by ligating the juxtaposed 3′-hydroxy and 5′-phosphate termini of a ssDNA molecule (Scheme 1a).[9,10] Another enzyme, CircLigase, can also be used to catalyze the end joining of a ssDNA bearing complementary ends (Scheme 1b).[11−13] However, the circularization yield in these reactions is relatively low because these approaches are also inherently capable of generating linear ligated products (LLP; the ligation of two or more of the same linear DNA molecules to create dimers, trimers, and multimers).[14,15] These side reactions occur because templated DNA synthesis is not programmed to offer high selectivity for intramolecular circularization over intermolecular ligation (there is no significant entropic difference between these two ligation reactions). Optimizing reaction conditions (e.g., Mg(II) concentration and temperature) and sequence design (e.g., stem length) can improve the yield and selectivity to some extent, but it cannot fundamentally exclude intermolecular ligation.[16,17] In addition, the base pairings near the end-joining site have to be carefully designed to reduce the negative effect of the size, structure, and topology on the circularization.[18,19]

We hypothesize that a possible solution to overcome the non-selective circularization issue is to develop a templating scaffold with the necessary structural arrangements that predominantly favor intramolecular circularization over intermolecular ligation. We further postulate that such a scaffold can be designed using unique DNA molecules that both bind the ligase enzyme to be employed for DNA circularization and act as the substrate for ligation by the ligase. In other words, it may be possible to first create a ligatable DNA aptamer for the ligase, which can then be engineered into a generalizable scaffold to guide the ligase to carry out selective intramolecular ligation.

Received: November 28, 2022
Published: January 19, 2023

https://doi.org/10.1021/jacs.2c12666
J. Am. Chem. Soc. 2023, 145, 2630−2637

Scheme 1. Traditional Strategies[a]

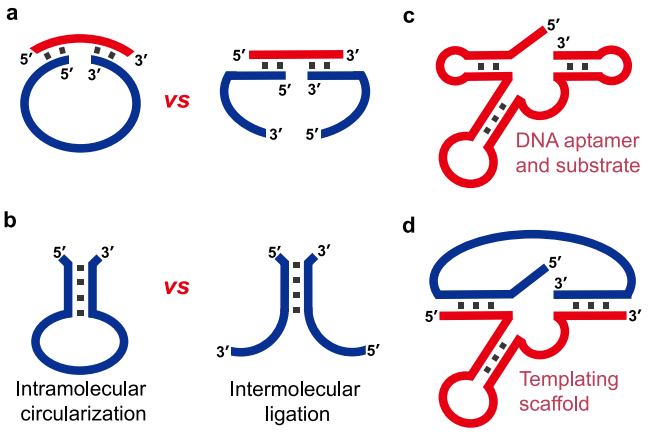

[a](a) T4 DNA ligase and (b) CircLigase-catalyzed intramolecular circularization of a ssDNA, both of which are inevitably accompanied by intermolecular ligation to produce linear ligated products. (c) Proposed ligatable DNA aptamer for the T4 DNA ligase, which also serves as a substrate that favors intramolecular circularization by the ligase. (d) Engineering the DNA aptamer into a templating DNA scaffold (red) to guide selective circularization of a second DNA molecule (blue).

To test this idea, we chose T4DL as the focal ligase, a DNA ligase widely used to perform DNA ligation reaction.[9,10] We hypothesize that there are special DNA molecules within the random sequence space that can recognize T4DL with high affinity and get ligated by T4DL, and such molecules can be isolated using the technique of in vitro selection (also known as SELEX).[20−22] As we will show in this report, we have successfully selected a ligatable DNA aptamer that has high affinity for T4DL (Scheme 1c). We have also carried out experiments to understand its secondary structure features, which lay the foundation for us to engineer a templating DNA scaffold, named TDS1, to allow T4DL to carry out selective intramolecular circularization of a ssDNA molecule of choice (Scheme 1d). Finally, We will demonstrate that TDS1 can be used to perform the high-yield selective synthesis of a series of circular DNA molecules, including a circular DNAzyme and a circular DNA aptamer that are designed to achieve specific bacterial detection.

RESULTS AND DISCUSSION

In Vitro Selection. The SELEX strategy includes three key enzymatic reactions (Figure 1): DNA circularization by T4DL, rolling circle amplification (RCA) by phi29 DNA polymerase (phi29DP), and restriction digestion by *EcoRV* (see Table S1 in the Supporting Information for details on all the DNA molecules used in this study).[23] The starting linear DNA library, DL1 contains, in the 5′ to 3′ direction, a 5′-phosphate, a 5′ 15-nt (nt: nucleotide) constant sequence element, a central 40-nt random region (N40), and a 3′ 17-nt constant sequence element. The last sequence element is designed to contain a 6-base pair stem and a 5-nt loop, which positions the 3′-hydroxy terminus of the library in duplex form to facilitate intramolecular ligation. In step i, DL1 ($\sim 10^{15}$) was incubated with T4DL in the selection buffer containing ATP: this step was aimed to isolate specific sequences named CTA undergoing circularization by T4DL. CTA was collected and subjected to RCA (RCA1; step ii) to produce complementary copies of CTA in large tandem repeats, which was digested

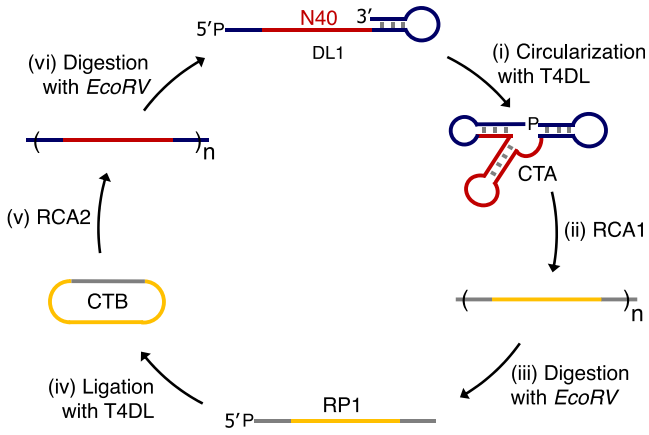

Figure 1. In vitro selection cycle employing multiple enzymatic reactions: DNA ligation with T4DL (steps i and iv), RCA (steps ii and iv), and restriction digestion with *EcoRV* (steps iii and vi).

with *EcoRV* into monomers (RP1; step iii). End-to-end ligation of RP1 was carried out in the presence of T4DL and a ssDNA splint, producing a new circular template named CTB (step iv). This was followed by another round of RCA (RCA2; step v) and restriction digestion (step vi) to regenerate the DNA pool for the next round of selection. A total of 14 SELEX cycles were performed. The 14th DNA pool was sequenced using our previously described protocols.[24]

Characterization of DAS1. The most dominant sequence, DAS1, accounts for ∼24%, indicating effective enrichment (Table S2). A secondary structure for DAS1 predicted by the mfold program (http://www.unafold.org/mfold/applications/dna-foldingform.php) is shown in Figure 2a. DAS1 contains one ss region (SS1), three short duplexes (P1, P2, and P3), three hairpin loops (L1, L2, and L3), and one interhelical unpaired element (J2/3). Figure 2b shows that DAS1 exhibited a yield of circularization (Y%) of 90% within 10 min for the

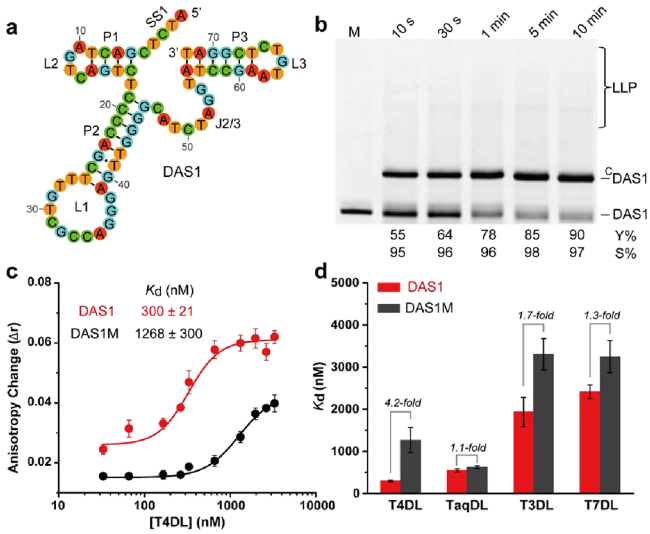

Figure 2. (a) Proposed secondary structure of DAS1. (b) Time-dependent intramolecular circularization of DAS1 by T4DL. Lane M: DAS1; LLP: linear ligated products; CDAS1: circular DAS1; Y%: circularization yield; S%: circularization selectivity. (c) Determination of K_d for DAS1 (or DAS1M) against T4DL using fluorescence anisotropy. (d) Comparison of K_d for DAS1 and DAS1M by four different DNA ligases: T4DL, TaqDL, T3DL, and T7DL.

https://doi.org/10.1021/jacs.2c12666
J. Am. Chem. Soc. 2023, 145, 2630−2637

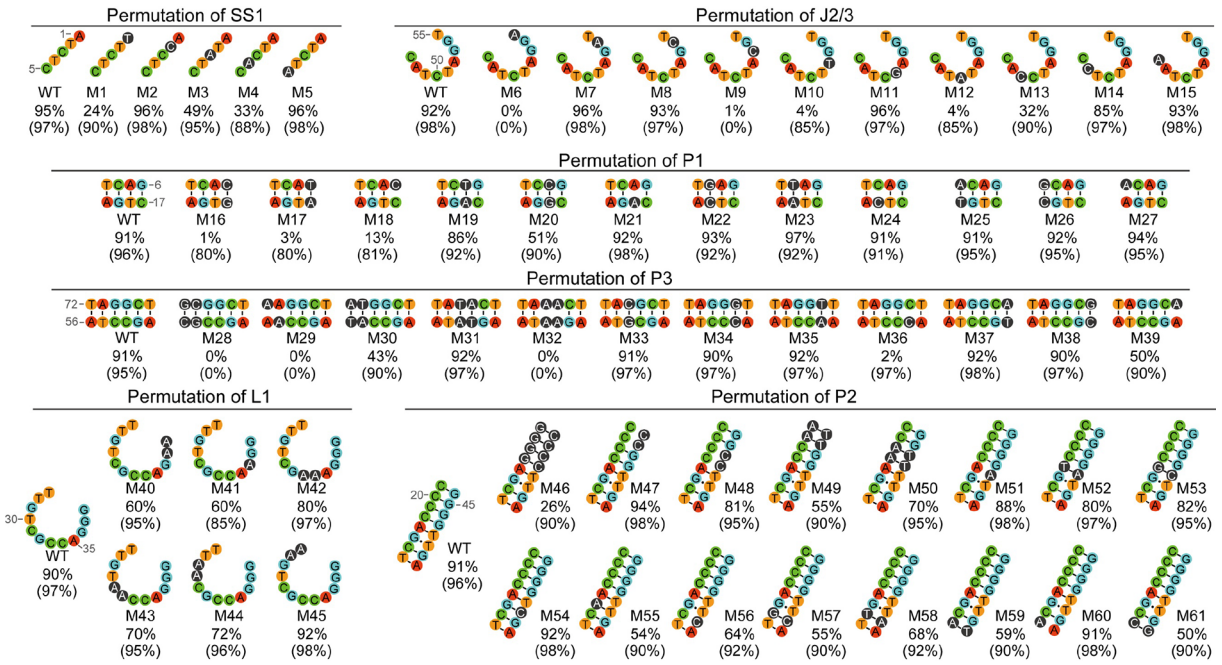

Figure 3. DAS1 with permutated SS1, J2/3, P1, P3, L1, and P2 elements. Nucleotides shown in black circles are the actual altered nucleotides in each construct in comparison to DAS1. WT: wild-type sequence. Y% is shown beneath each construct, with the S% in parentheses.

formation of its monomeric ring, ^{C}DAS1. No ^{C}DAS1 was observed in the absence of T4DL (Figure S1). We also used the term "circularization selectivity" (S%) to describe the selectivity of DAS1 for intramolecular circularization over intermolecular ligation. Remarkably, S% of DAS1 was determined to be 97%, indicating that DAS1 nearly exclusively favors circularization. Furthermore, DAS1 exhibited the highest Y% and S% compared with the other top four sequences (Figure S2), and therefore, we chose DAS1 as the focal molecule in this study.

To further evaluate the performance in terms of Y% and S%, we carried out three additional experiments. First, DAS1 was used as a substrate for T4DL in a standard ligation reaction where a DNA splint (DS1) was used to template the 5′ and 3′ ends of DAS1 for circularization. It was observed that S% is highly dependent on the stoichiometric ratio between the splint and the substrate (Figure S3): S% were found to be 75, 66, and 59% when the ratios of DS1:DAS1 were set to be 1:1, 1.5:1, and 3:1, respectively. However, Y% was observed to be 37−40%, regardless of the ratio. Second, for circularization of DAS1 by CircLigase, we observed a Y% of only 19% and an S% of 72% in a reaction time of 10 min (Figure S4). In the third experiment, a different DNA ligase, Taq DNA ligase (TaqDL), was used to replace T4DL, which produced a Y% of only 7% and an S% of 70% (Figure S5). Note that both CircLigase and TaqDL are active at elevated temperatures (45 and 60 °C for CircLigase and TaqDL, respectively), which appears to reduce the formation of polymeric byproducts and favor circularization. Taken together, these results demonstrate that DAS1 is a highly specific substrate for T4DL and also suggest that DAS1 adopts a structural arrangement that favors intramolecular circularization by T4DL.

The specific binding between DAS1 and T4DL was examined by measuring the dissociation constant (K_d) using fluorescence anisotropy (Figure 2c). T4DL has been shown to have micromolar affinity for nonspecific DNA binding.[25] However, T4DL showed significantly better binding affinity for DAS1 with a K_d of 300 ± 21 nM while exhibiting an over 4-fold affinity reduction for mutant DAS1 (DAS1M in which the nucleotides in L2 and J2/3 were mutated into adenosine residues), with a K_d of 1268 ± 300 nM. The binding affinity for DAS1 and DAS1M was also measured for three other DNA ligases: TaqDL (Figure S6a), T3 DNA ligase (T3DL; Figure S6b), and T7 DNA ligase (T7DL; Figure S6c). TaqDL showed good affinity for (K_d = 550 ± 38 nM) but poor selectivity for DAS1 over DAS1M (only 1.1-fold difference in K_d. The affinity for DAS1 by T3DL (K_d = 1936 ± 347 nM) and T7DL (K_d = 2415 ± 163 nM) was much poorer; the selectivity for DAS1 over DAS1M by both T3DL and T7DL was also significantly reduced (1.7- and 1.3-fold, respectively, Figure 2d and Figure S6). Taken together, these results suggest that DAS1 has been successfully selected both as an aptamer for T4DL and as an optimal substrate for T4DL-mediated circularization (i.e., intramolecular ligation).

To assess the essentiality of each nucleotide within DAS1, 61 mutant constructs of DAS1 were examined (Figure 3 and Figure S7). Within SS1, A1, C3, and T4 are important for high Y% as mutation to each of them significantly reduced Y% (M1, M3, and M4). In contrast, the remaining two nucleotides (T2 and C5) can be mutated (M2 and M5). Within the J2/3 element, T55, G53, A52, C50, and T49 are important nucleotides and mutation to any one of them drastically reduced Y% (M10, M12, and M13) or both Y% and S% (M6 and M9). However, G54, T51, A48, and C47 can tolerate mutations. For P1, mutating the G6-C17 pair into the C-G pair (M16), T-A pair (M17), or C-C mismatch (M18) significantly reduced the Y%. Substituting the A7-T16 pair with a T-A pair (M19) or even an A-A mismatch (M21) did not considerably impact either Y% and S%; however, Y% was decreased by half with C-G pair substitution (M20). Mutations of the C8-G15 pair into the G-C pair (M22), T-A pair (M23), or even C-C mismatch (M24) were well tolerated. Similarly, altering the T9-A14 pair to an A-T pair (M25), a G-C pair (M26), or A-A mismatch (M27) did not cause notable reductions in Y% and S

https://doi.org/10.1021/jacs.2c12666
J. Am. Chem. Soc. 2023, 145, 2630−2637

%. For P3, changing the T72-A56 and A71-T57 pairs to the A-T and T-A pairs (M30) caused the reduction of Y% by half; however, when they were changed to the G-C and C-G pairs (M28), or two A-A mismatch pairs (M29), no activity was observed. G70-C58 and G69-C59 pairs can be substituted with T-A and A-T pairs without any change in Y% and S% (M31); however, ligation activity was completely lost when these two base pairs were substituted with two A-A mismatch pairs (M32). The C68-G60 pairs could be changed to a G-C pair (M34) or a T-A pair (M35) but not a C-C mismatch (M36). For the T67-A61 pair, the substitution with an A-T pair (M37) or a G-C pair (M38) can be tolerated; however, the substitution with an A-A mismatch (M39) reduced Y% by half. For L1, the identities of the 10 nucleotides from G29 to G38 are important to the optimal function of DAS1 because mutating any of these nucleotides (M40-M44) caused a noticeable reduction on Y%. However, the remaining two nucleotides, T32 and T33, can tolerate mutations (M45). For P2, when the first four C-G pairs were flipped to G-C pairs (M46), a significant decrease in Y% was obtained (Y% = 26%). Changing the top two G-C pairs to two A-T pairs (M49) or changing the next two G-C pairs to two A-T pairs (M50) or two C-C mismatch pairs (M48) also caused noticeable Y% reduction. Interestingly, substituting the two G-C pair with two C-C mismatch pairs (M47) was well tolerated. The A17-T42 pair could also tolerate, to a large extent, the change to a T-A (M52) or G-C pair (M53) or even A-A mismatch (M51). When the G16·T41 wobble pair was mutated into a G-C pair (M54), no reduction in Y% was observed; however, if the wobble pair was altered to the A-T pair (M55), then Y% dropped by half. The C15-G40 pair is also important for the optimal function of DAS1 as substituting it with a G-C pair (M57), a T-A pair (M58), or a C-C mismatch (M56) dropped Y% to ~60%. Finally, while replacing the T14-A39 pair with an A-T pair (M59) or a G-C pair (M61) reduced Y% to 50−60%, it can tolerate an A-A mismatch (M60). Taken together, these results support the following conclusions: (i) several nucleotides located within the SS1 and J2/3 elements are critically involved in the function of DAS1 and cannot tolerate base mutations; (ii) a few putative base pairs within P1 and P3 are highly important to the function of DAS1 and their identities cannot be altered while other putative base pairs can either be substituted with other base pairs or tolerate mismatches; and (iii) none of the nucleotides within L1 or the base pairs within P2 (both elements are distal to the ligation junction) is not essential to the function of DAS1 but many contribute to the optimal function of DAS1.

Based on the mutational analysis, we also speculate that weak intramolecular interactions occur between J2/3 and SS1 that position T4DL for binding and ligation. This was confirmed experimentally: when DAS1 was mutated to DAS1-I, which was designed to create a very strong Watson−Crick duplex between SS1, J2/3, and part of P1 in DAS1 (Figure 4a), the Y% and S% were decreased to 45 and 81%, respectively (Figure 4b). This observation strongly suggests that the SS1-J2/3 weak interactions play significant roles in the selective intramolecular ligation.

Converting DAS1 into a Templating DNA Scaffold for the Selective Synthesis of Circular DNA Molecules. The proposed secondary structure of DAS1 and finding that its SS1 and J2/3 elements are important for the high Y% and S% immediately imply that it can be converted into a templating DNA scaffold to allow T4DL to circularize a second DNA

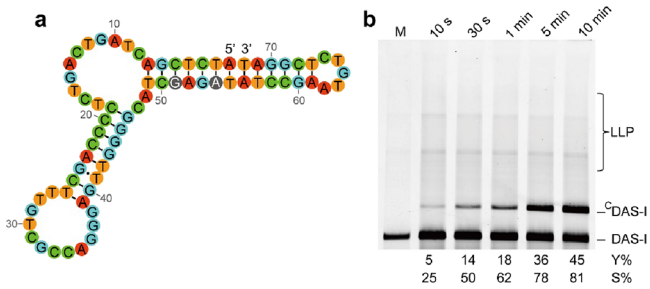

Figure 4. (a) Proposed secondary structure of DAS1-I. Nucleotides shown in two black circles highlight two nucleotides in DAS1-I mutated from DAS1. (b) Time-dependent circularization of DAS1-I by T4DL. Lane M: DAS1-I; LLP: linear ligated products; ^{C}DAS1-I: circular DAS1-I.

molecule (Scheme 1d). Specifically, we postulate that keeping SS1, J2/3, P2, and L2 unchanged and rearranging P1-L1 and P3-L3 elements to deliver bimolecular interactions involving the trans-acting DAS1 and the second DNA molecule will produce a DAS1-derived templating scaffold (which we name TDS1) to circularize an external DNA molecule.

We first demonstrate this possibility through the synthesis of a circular version of EC1, a previously described RNA-cleaving DNAzyme whose activity can be activated by *Escherichia coli*.[26,27] Two modifications were made to the sequence of EC1: (i) its 5′ end was expanded to contain the needed SS1 element; (ii) two binding arms were created to allow the formation of P1 and P3 with a trans-acting version of DAS1 named TDS1.T1 (Figure 5a). Figure 5b shows that circular EC1 (^{C}EC1) was obtained with a Y% of 94% and an S% of 92% within 10 min. For comparison, the traditional DNA splint strategy was less effective (Figure S8, Y% = 82%; S% =

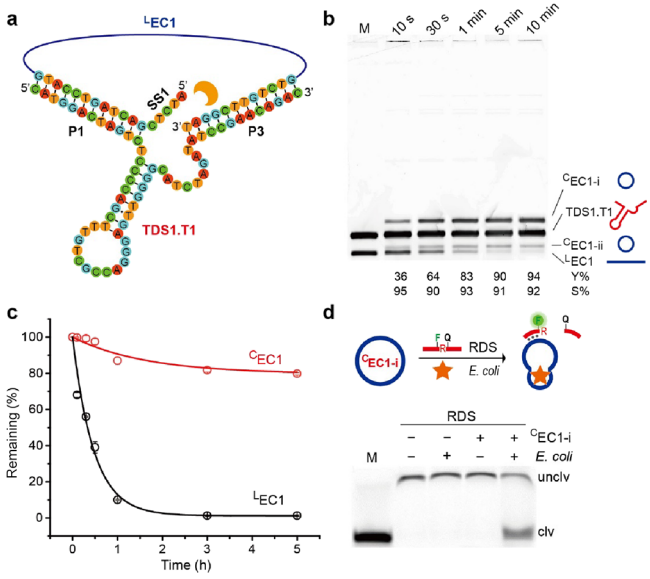

Figure 5. (a) Schematics of trans-acting TDS1.T1-directed circularization of ^{L}EC1 by T4DL. (b) Time-dependent synthesis of ^{C}EC1. The suspected ^{C}EC1 is marked as ^{C}EC1-N (N = i or ii, representing sister ^{C}EC1 from the same EC1). Lane M, markers made of TDS1.T1 and ^{L}EC1. (c) Biostability of ^{L}EC1 and ^{C}EC1 in CIM. (d) 10% dPAGE analysis of the cleavage of RDS by ^{C}EC1-i and *E. coli*. F = fluorescein-dT, Q = dabcyl-dT, R = adenosine ribonucleotide, unclv = uncleaved, clv = cleaved.

https://doi.org/10.1021/jacs.2c12666
J. Am. Chem. Soc. 2023, 145, 2630−2637

81%). Note that two forms of ^{C}EC1 were observed, a slower-moving species ^{C}EC1-i (major product) and a faster-moving species ^{C}EC1-ii (minor product). To confirm that ^{C}EC-i and ^{C}EC-ii were two topological isomers, we performed RCA reactions with gel-purified ^{C}EC1-i and ^{C}EC1-ii. It was observed that RCA products (RP) were produced with both ^{C}EC1-i and ^{C}EC1-ii (Figure S9). Furthermore, each RP was expected to contain a recognition sequence (GATATC) for the restriction enzyme *EcoRV*. Upon digestion with *EcoRV*, each RP indeed produced an identical DNA banding pattern indicative of a monomer, dimer, and other higher-ordered DNA repeats (Figure S10).

The crude intracellular mixture (CIM) prepared from *E. coli* is often used as the target for the EC1 DNAzyme,[28−31] and therefore, we tested the molecular integrity of linear EC1 (^{L}EC1) and ^{C}EC1 in such samples (Figure 5c). As much as 90% of the ^{L}EC1 was digested in 1 h, only 13% of ^{C}EC1 was lost. This result indicated that ^{C}EC1 was more desirable than its linear form for bacterial detection. We then examined RNA cleavage reactions with ^{C}EC1 (Figure 5d). In the presence of *E. coli*, ^{C}EC1-i was indeed able to cleave an RNA-containing DNA sequence (RDS) in which a ribonucleotide (R) is flanked immediately by two deoxyribonucleotides, one containing a fluorophore (F) and the other a quencher (Q).

The cleavage reactions, in response to varying concentrations of *E. coli*, were also monitored by real-time fluorescence measurement (Figure 6a). This sensor can

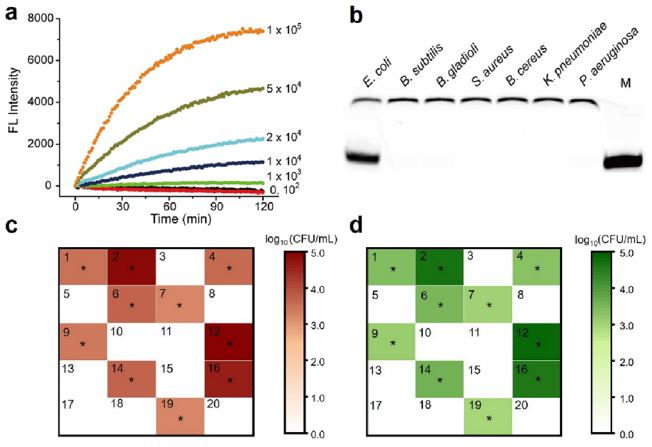

Figure 6. (a) Real-time fluorescence monitoring of ^{C}EC1-i/RDS at various *E. coli* concentrations (cells/mL). (b) 10% dPAGE analysis of the responses of ^{C}EC1-i/RDS to various microbes. Quantification of *E. coli* in 20 clinical urine samples using (c) ^{C}EC1-i/RDS and (d) culture-based methods.

achieve a limit of detection (LOD) of 10^3 cells/mL without cell culture. This represents a 10-fold improvement in LOD over the traditional ^{L}EC1 sensor.[26,27] The increased detection sensitivity was likely due to the enhanced biological stability of ^{C}EC1 vs ^{L}EC1. We also investigated the sensitivity using urine samples spiked with different concentrations of *E. coli*. It was able to detect *E. coli* at a concentration of 10^3 cells/mL (Figure S11). Besides the high sensitivity, this sensor also exhibited excellent selectivity for its cognate target (Figure 6b). None of the several arbitrarily chosen bacteria (including *Bacillus subtilis*, *Burkholderia gladioli*, *Staphylococcus aureus*, *Bacillus cereus*, *Klebsiella pneumoniae*, and *Pseudomonas aeruginosa*) can activate ^{C}EC1.

To investigate the potential clinical applicability of this sensor in diagnosis of urinary tract infections (UTIs), we analyzed 20 clinical urine samples. As shown in Figure 6c, the DNAzyme assay was able to detect ≥10^3 CFU/mL *E. coli* in seven urine samples (namely, ID 1, 4, 6, 7, 9, 14, and 19) and ≥10^4 CFU/mL *E. coli* in three samples (namely, ID 2, 12, and 16). A clinical threshold of 10^3 CFU/mL was commonly used by clinicians to decide on UTI treatment.[32] Therefore, our sensor is promising for UTI diagnosis. As a control, we also carried out *E. coli* detection for the same biological sample set using the traditional bacterial culture method (Figure S12). The result provided in Figure 6d shows that both the bacterial culture and the DNAzyme method produced comparable *E. coli* concentrations in these clinical samples. However, the sample-to-result time was less than 2.5 h for our sensor, compared with 15 h needed for the currently used culture-based methods.

The utility of TDS1 for circularizing external DNA molecules was further demonstrated by the synthesis of additional circular DNA molecules. First, TDS1 was used for circularization of a set of random-sequence DNA pools. Specifically, the trans-acting TDS1.T1 was used to direct circularization of five linear DNA pools named DP-10, DP-20, DP-40, DP-60, and DP-80, which contain random regions of 10, 20, 40, 60, and 80 nucleotides, respectively (Figure S13). As shown in Figure 7a, the circularization selectivity remained

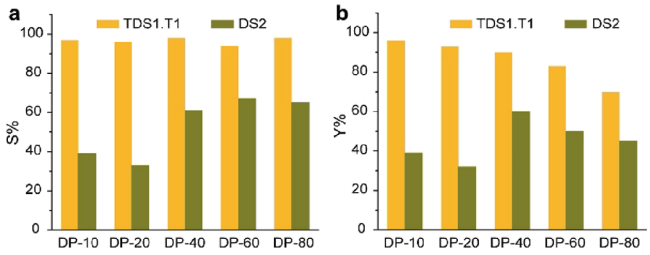

Figure 7. Comparison of TDS1.T1 and DS2-mediated circularization of different-sized DNA pools by T4DL. (a) Circularization selectivity (S%) and (b) circularization yield (Y%).

at high levels (S% > 94%; 10 min reaction), regardless of the DNA size. The circularization yields slightly decreased with the increase in DNA length: 96, 93, 90, 83, and 70% for DP-10, DP-20, DP-40, DP-60, and DP-80, respectively (Figure 7b and Figure S13; 10 min reaction). In contrast, the conventional DNA splint-based strategy was much less effective, with S% varying between 33 and 67% and Y% fluctuating between 32 and 60% (Figure 7b and Figure S14; 10 min reaction). Circular DNA libraries have been used as the starting pools to select circular DNA aptamers and DNAzymes that are highly functional in biological samples,[12,33,34] and therefore, TDS1 should be useful for circular random DNA library synthesis for future SELEX experiments.

In the second experiment, TDS1.T1 was employed for circularizing a linear 8-17 DNAzyme, named ^{L}8-17Dz, a widely studied RNA-cleaving DNAzyme.[35] The TDS1.T1-based strategy produced a Y% of 94% and an S% of 98% (Figure S16a; 10 min reaction). For comparison, a Y% of 72% and an S % of 75% were obtained for the conventional DNA splint-based strategy (Figure S16b). Taken together, these results highlight the enticing advantage of TDS1-based circularization in terms of both reaction yield and circularization selectivity.

https://doi.org/10.1021/jacs.2c12666
J. Am. Chem. Soc. 2023, 145, 2630−2637

We also performed the DNA splint-mediated circularization in polyethylene glycol (PEG)-containing conditions to see if PEG can improve the intramolecular ligation.[36] PEG with three different molecular weights (PEG 200, PEG 1000, and PEG 8000) was tested for circularizing the DNA library DP-20 (Figure S15). PEG was found to improve both Y% and S% to some extent; for example, Y% and S% in the PEG1000-containing buffer were found to be 47 and 50% (Figure S15c) respectively, compared to 32 and 33% in the PEG-free buffer, respectively (Figure S14). However, these values are still much smaller than the Y% (93%) and S% (96%) values observed with TDS1.T1 mediated reaction (Figure 7).

Rational Design of the Circular DNA Aptamer Reporter. The multiple examples provided above illustrate the utility of TDS1 in the preparation of circular DNA molecules with high yield and high selection for intramolecular ligation vs intermolecular ligation. We further postulate that TDS1 can also be combined with a functional nucleic acid to achieve direct biosensing as we will demonstrate hereafter with the design of a circular DNA aptamer reporter for the detection of toxin B, an established biomarker for diagnosing *Clostridium difficile* infections.[24] As illustrated in Figure 8a, the

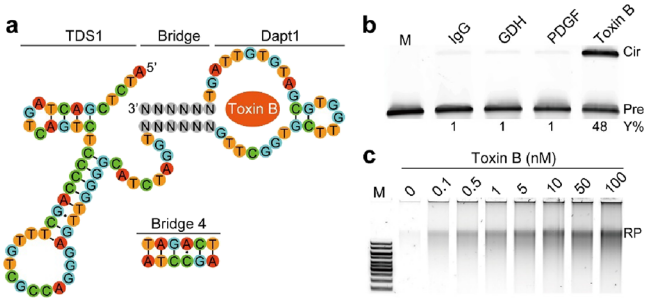

Figure 8. (a) DNA sequences used for the construction of a circular aptamer reporter (N = A, T, C, and G) and the sequence of bridge 4. (b) Specificity of target response. Pre: linear molecular precursors; Cir: circularized products. (c) Agarose gel analysis of RP in RCA reactions initiated by toxin B (0.1−100 nM). Lane M, DNA ladders ranging from 1 to 10 kbp.

reporter is made of an anti-toxin B DNA aptamer (Dapt1) and a TDS1 that are conjoined by a short duplex bridge composed of 12 nucleotides (represented by the 12 N residues in Figure 8a). The idea is that in the absence of toxin B, the bridge is not strong enough to permit circularization. However, the presence of toxin B will stabilize the bridge, triggering circularization. The resultant circular products can then serve as the template for RCA.

The key component of the system is the ligand-responsive bridge element. Four different bridges, designated as bridge 1−4, were examined (Figure S17). The sensor carrying bridge 4 produced negligible circularization in the absence of toxin B but was able to produce significant amounts of circular DNA in the presence of toxin B. The amount of circular DNA was found to increase with rising concentrations of toxin B (Figure S18). In contrast, only small amounts of circular DNA were observed when the reporter was tested with unintended targets (Figure 8b), including immunoglobin G (IgG), glutamate dehydrogenase (GDH, a general antigen of *C. difficile*), and platelet-derived growth factor (PDGF). We also examined the feasibility of performing quantitative analysis of toxin B using RCA. As shown in Figure 8c, a limit of detection (LOD, defined as 3σ, σ = standard deviation of the blank samples) of 0.1 nM was achieved within 30 min, including an activation time of 15 min, a cyclization time of 5 min, and an RCA time of 10 min.

CONCLUSIONS

In summary, we derived a DNA aptamer that binds T4DL and acts as the substrate for ligation by the DNA ligase. This DNA aptamer was found to adopt an intricate secondary structure that favors intramolecular circularization over intermolecular ligation by T4DL. Based on the structural information, we engineered this aptamer into a general-purpose templating DNA scaffold, named TDS1, to guide the ligase to execute selective intramolecular circularization of a second single-stranded DNA molecule. TDS1 was employed to synthesize a series of circular ssDNA molecules at high yield and excellent circularization selectivity. For example, TDS1 was used to synthesize a circular RNA-cleaving DNAzyme that can be activated by *E. coli*, and the resultant circular DNAzyme showed improved resistance to degradation by nucleases in biological samples and achieved the sensitive detection of *E. coli* in urine samples. TDS1 was also used to construct a circular DNA aptamer that binds toxin B of *C. difficile* in a biosensing assay that can specifically transduce toxin B presence into DNA amplicons for detection. We envision that the strategy presented in this study will open new opportunities for future exploitation of circular functional nucleic acids in chemical biology, medical diagnostics, computing, and biosensing.

ASSOCIATED CONTENT

Supporting Information

The Supporting Information is available free of charge at https://pubs.acs.org/doi/10.1021/jacs.2c12666.

Experimental section, supporting tables including sequences of DNA oligonucleotides, circularization of DAS1 without T4DL, time-dependent intramolecular circularization of DAS2, DAS3, DAS4, and DAS5, circularization of DAS1 by T4DL in the presence of DS1, circularization of DAS1 by CircLigase and TaqDL, determination of K_d of TaqDL, T3DL, and T7DL for DAS1 and DAS1M, permutations of SS1, J2/3, P1, P3, L1, and P2 elements in DAS1, circularization of ^{L}EC1 by T4DL in the presence of DS2, RCA reactions, digestion of RCA products, urine sample detection, traditional bacterial culture result, trans-acting TDS1.T1-directed circularization of DNA pools by T4DL, DS2-mediated circularization of DNA pools by T4DL, circularization of DP-20 by T4DL in PEG-containing buffer, circularization of ^{L}8-17Dz by T4DL, and responses of different reporters (PDF)

AUTHOR INFORMATION

Corresponding Authors

Yingfu Li − *Department of Biochemistry and Biomedical Sciences, McMaster University, Hamilton, Ontario L8S4K1, Canada;* orcid.org/0000-0002-7533-6743; Email: liying@mcmaster.ca

Meng Liu − *School of Environmental Science and Technology, Key Laboratory of Industrial Ecology and Environmental Engineering (Ministry of Education), Dalian POCT Laboratory, Dalian University of Technology, Dalian,*

https://doi.org/10.1021/jacs.2c12666
J. Am. Chem. Soc. 2023, 145, 2630−2637

Liaoning 116024, China; orcid.org/0000-0003-3114-9003; Email: mliu@dlut.edu.cn

Authors

Yu Yan − *School of Environmental Science and Technology, Key Laboratory of Industrial Ecology and Environmental Engineering (Ministry of Education), Dalian POCT Laboratory, Dalian University of Technology, Dalian, Liaoning 116024, China*

Dingran Chang − *Department of Biochemistry and Biomedical Sciences, McMaster University, Hamilton, Ontario L8S4K1, Canada;* orcid.org/0000-0002-3127-8668

Yongbin Xu − *Department of Bioengineering, College of Life Science, Dalian Nationalities University, Dalian, Liaoning 116600, China;* orcid.org/0000-0002-6591-9320

Yangyang Chang − *School of Environmental Science and Technology, Key Laboratory of Industrial Ecology and Environmental Engineering (Ministry of Education), Dalian POCT Laboratory, Dalian University of Technology, Dalian, Liaoning 116024, China*

Qiang Zhang − *School of Bioengineering, Dalian University of Technology, Dalian, Liaoning 116024, China*

Quan Yuan − *State Key Laboratory of Chemo/Biosensing and Chemometrics, College of Chemistry and Chemical Engineering, Institute of Chemical Biology and Nanomedicine, Hunan University, Changsha 410082, China;* orcid.org/0000-0002-3085-431X

Bruno J. Salena − *Department of Medicine, McMaster University, Hamilton, Ontario L8S4K1, Canada*

Complete contact information is available at: https://pubs.acs.org/10.1021/jacs.2c12666

Notes

The authors declare no competing financial interest.

■ ACKNOWLEDGMENTS

This work was supported by the National Natural Science Foundation of China (NSFC; grant no. 21922601), the Fundamental Research Funds for the Central Universities (DUT20YG123), and the Natural Sciences and Engineering Research Council of Canada (RGPIN-2020-06401).

■ REFERENCES

(1) Kool, E. T. Circular oligonucleotides: new concepts in oligonucleotide design. *Annu. Rev. Biophys. Biomol. Struct.* **1996**, *25*, 1−28.

(2) Li, J.; Mohammed-Elsabagh, M.; Paczkowski, F.; Li, Y. Circular nucleic acids: discovery, functions and applications. *ChemBioChem* **2020**, *21*, 1547−1566.

(3) Nilsson, M.; Malmgren, H.; Samiotaki, M.; Kwiatkowski, M.; Chowdhary, B. P.; Landegren, U. Padlock probes: circularizing oligonucleotides for localized DNA detection. *Science* **1994**, *265*, 2085−2088.

(4) Jester, S.; Famulok, M. Mechanically interlocked DNA nanostructures for functional devices. *Acc. Chem. Res.* **2014**, *47*, 1700−1709.

(5) Valero, J.; Lohmann, F.; Famulok, M. Interlocked DNA topologies for nanotechnology. *Curr. Opin. Biotechnol.* **2017**, *48*, 159−167.

(6) Mohsen, M. G.; Kool, E. T. The discovery of rolling circle amplification and rolling circle transcription. *Acc. Chem. Res.* **2016**, *49*, 2540−2550.

(7) Cheulhee Jung, C.; Ellington, A. D. Diagnostic applications of nucleic acid circuits. *Acc. Chem. Res.* **2014**, *47*, 1825−1835.

(8) Ali, M. M.; Li, F.; Zhang, Z.; Zhang, K.; Kang, D. K.; Ankrum, J. A.; Le, X. C.; Zhao, W. Rolling circle amplification: a versatile tool for chemical biology, materials science and medicine. *Chem. Soc. Rev.* **2014**, *43*, 3324−3341.

(9) Kool, E. T. Recognition of DNA, RNA, and proteins by circular oligonucleotides. *Acc. Chem. Res.* **1998**, *31*, 502−510.

(10) Tomkinson, A. E.; Vijayakumar, S.; Pascal, J. M.; Ellenberger, T. DNA ligases: structure, reaction mechanism, and function. *Chem. Rev.* **2006**, *106*, 687−699.

(11) Lin, C.; Wang, X.; Liu, Y.; Seeman, N. C.; Yan, H. Rolling circle enzymatic replication of a complex multi-crossover DNA nanostructure. *J. Am. Chem. Soc.* **2007**, *129*, 14475−14481.

(12) Gu, H.; Furukawa, K.; Weinberg, Z.; Berenson, D. F.; Breaker, R. R. Small, highly active DNAs that hydrolyze DNA. *J. Am. Chem. Soc.* **2013**, *135*, 9121−9129.

(13) Du, X.; Zhong, X.; Li, W.; Li, H.; Gu, H. Retraining and optimizing DNA-hydrolyzing deoxyribozymes for robust single- and multiple-turnover activities. *ACS Catal.* **2018**, *8*, 5996−6005.

(14) Doherty, A. J.; Dafforn, T. R. Nick recognition by DNA ligases. *J. Mol. Biol.* **2000**, *296*, 43−56.

(15) Lehman, I. R. DNA ligase: structure, mechanism, and function. *Science* **1974**, *186*, 790−797.

(16) An, R.; Li, Q.; Fan, Y.; Li, J.; Pan, X.; Komiyama, M.; Liang, X. Highly efficient preparation of single-stranded DNA rings by T4 ligase at abnormally low Mg(II) concentration. *Nucleic Acids Res.* **2017**, *45*, No. e139.

(17) Cui, Y.; Han, X.; An, R.; Zhang, Y.; Cheng, K.; Liang, X.; Komiyama, M. Terminal hairpin in oligonucleotide dominantly prioritizes intramolecular cyclization by T4 ligase over intermolecular polymerization: an exclusive methodology for producing ssDNA rings. *Nucleic Acids Res.* **2018**, *46*, No. e132.

(18) Liu, D.; Chen, G.; Akhter, U.; Cronin, T. M.; Weizmann, Y. Creating complex molecular topologies by configuring DNA four-way junctions. *Nat. Chem.* **2016**, *8*, 907−914.

(19) Liu, D.; Shao, Y.; Chen, G.; Tswe-Dunh, Y.; Piccirilli, J. A.; Weizmann, Y. Synthesizing topological structures containing RNA. *Nat. Commun.* **2017**, *8*, 14936.

(20) Ellington, A. D.; Szostak, J. W. In vitro selection of RNA molecules that bind specific ligands. *Nature* **1990**, *346*, 818−822.

(21) Tuerk, C.; Gold, L. Systematic evolution of ligands by exponential enrichment: RNA ligands to bacteriophage T4 DNA polymerase. *Science* **1990**, *249*, 505−510.

(22) Robertson, D. L.; Joyce, G. F. Selection in vitro of an RNA enzyme that specifically cleaves single-stranded DNA. *Nature* **1990**, *344*, 467−468.

(23) Mao, Y.; Liu, M.; Tram, K.; Gu, J.; Salena, B. J.; Jiang, Y.; Li, Y. Optimal DNA templates for rolling circle amplification revealed by in vitro selection. *Chem. − Eur. J.* **2015**, *21*, 8069−8074.

(24) Liu, M.; Wang, J.; Chang, Y.; Zhang, Q.; Chang, D.; Hui, C. Y.; Brennan, J. D.; Li, Y. In vitro selection of a DNA aptamer targeting degraded protein fragments for biosensing. *Angew. Chem., Int. Ed.* **2020**, *59*, 7706−7710.

(25) Shi, K.; Bohl, T. E.; Park, J.; Zasada, A.; Malik, S.; Banerjee, S.; Tran, V.; Li, N.; Yin, Z.; Kurniawan, F.; Orellana, K.; Aihara, H. T4 DNA ligase structure reveals a prototypical ATP-dependent ligase with a unique mode of sliding clamp interaction. *Nucleic Acids Res.* **2018**, *46*, 10474−10488.

(26) Ali, M. M.; Aguirre, S. D.; Lazim, H.; Li, Y. Fluorogenic DNAzyme probes as bacterial indicators. *Angew. Chem., Int. Ed.* **2011**, *50*, 3751−3754.

(27) Aguirre, S.; Ali, M.; Salena, B.; Li, Y. A sensitive DNA enzyme-based fluorescent assay for bacterial detection. *Biomolecules* **2013**, *3*, 563−577.

(28) Liu, M.; Zhang, Q.; Li, Z.; Gu, J.; Brennan, J. D.; Li, Y. *Nat. Commun.* **2016**, *7*, 12074.

(29) Liu, M.; Zhang, Q.; Chang, D.; Gu, J.; Brennan, J. D.; Li, Y. A DNAzyme feedback amplification strategy for biosensing. *Angew. Chem., Int. Ed.* **2017**, *56*, 6142−6146.
(30) Liu, M.; Zhang, Q.; Kannan, B.; Botton, G. A.; Yang, J.; Soleymani, L.; Brennan, J. D.; Li, Y. Self-assembled functional DNA superstructures as high-density and versatile recognition elements for printed paper sensors. *Angew. Chem., Int. Ed.* **2018**, *57*, 12440−12443.
(31) Tram, K.; Kanda, P.; Salena, B. J.; Huan, S.; Li, Y. Translating bacterial detection by DNAzymes into a litmus test. *Angew. Chem., Int. Ed.* **2014**, *53*, 12799−12802.
(32) Flores-Mireles, A. L.; Walker, J. N.; Caparon, M.; Hultgren, S. J. Urinary tract infections: epidemiology, mechanisms of infection and treatment options. *Nat. Rev. Microbiol.* **2015**, *13*, 269−284.
(33) Mao, Y.; Gu, J.; Chang, D.; Wang, L.; Yao, L.; Ma, Q.; Luo, Z.; Qu, H.; Li, Y.; Zheng, L. Evolution of a highly functional circular DNA aptamer in serum. *Nucleic Acids Res.* **2020**, *48*, 10680−10690.
(34) Liu, M.; Yin, Q.; Chang, Y.; Zhang, Q.; Brennan, J. D.; Li, Y. In vitro selection of circular DNA aptamers for biosensing applications. *Angew. Chem., Int. Ed.* **2019**, *58*, 8013−8017.
(35) Santoro, S. W.; Joyce, G. F. A general purpose RNA-cleaving DNA enzyme. *Proc. Natl. Acad. Sci. U. S. A.* **1997**, *94*, 4262−4266.
(36) Hayashi, K.; Nakazawa, M.; Ishizaki, Y.; Hiraoka, N.; Obayashi, A. Regulation of inter- and Intramolecular Ugation with T4 DNA ligase in the presence of polyethylene glycol. *Nucleic Acids Res.* **1986**, *14*, 7617−7631.

https://doi.org/10.1021/jacs.2c12666
J. Am. Chem. Soc. 2023, 145, 2630−2637